HIGH SCHOOL EDITION
Journal of Student Research
Volume 13 Issue 1 (2024)

Fusing Age-Guided Features in Convolutional Neural Network for Accurate Retinal Disease Diagnosis

Jiwoo Lee[1] and Nicole Kim[#]

[1]Thomas Jefferson High School for Science and Technology, USA
[#]Advisor

ABSTRACT

Eye diseases are a significant global health issue, impacting millions of people and potentially leading to serious side effects, such as vision loss, in the absence of proper treatment and early diagnosis. Nevertheless, the traditional method faces several challenges, including time-consuming procedures, susceptibility to human error, and workforce shortage in impoverished areas. There is a growing demand for accurate automation systems to address these issues. To address the aforementioned problem, extensive research has been conducted, leveraging machine learning techniques to develop an eye disease recognition system. Previous studies demonstrated the potential of convolutional neural networks in diagnosing the patient. However, these methods often suffer from inaccuracies and limitations in targeting a wide range of diseases, rendering them less practical. Thus, I propose a novel eye disease recognition framework to overcome the previously mentioned shortage. I introduce an age-guided approach to improve the accuracy of the disease diagnosis process. The research results demonstrate the outperformance of the proposed model, achieving state-of-the-art performance with an accuracy of 84% on a publicly available eye disease dataset.

Introduction

Problem Definition

Eye diseases are a category of medical conditions that affect the eye. It is a significant global health concern which affects millions of people and leads to severe side effects. Numerous challenges, including early and accurate diagnosis of various conditions, are present in treating eye diseases. However, traditional diagnostic methods often fail to overcome these challenges because of their trait of heavily relying on the expertise of ophthalmologists.

Recent advances in machine learning-based computer vision techniques have shown promising performance. There have been several attempts to apply these techniques to diagnosis of eye diseases from retinal images. In particular, convolutional neural networks have shown outstanding performance, especially in the analysis of digital images like retinal images.

Previous Method

To address this issue, there has been a considerable amount of research on diagnosis systems based on retinal images. Zhang et al. (Zhang et al. 2021) proposed a deep-learning algorithm to detect kidney disease and type two diabetes. Rim et al. (Rim et al. 2020) proposed a deep-learning algorithm to predict systemic biomarkers.

Cen et al. (Cen et a. 2021) proposed a detection system to detect 39 fundus diseases. These methods demonstrated the feasibility of diagnosing eye-related diseases from retinal images using machine learning.

Yet, the previous research does not provide accurate results because they tend to be biased toward the training set. Their approach cannot be extended to real-world applications due to its poor results. To solve this, I propose an eye disease diagnosis system with numerous target diseases and high performance.

Proposed Method

In this research, I aim to explore the application of convolutional neural networks in diagnosing various eye diseases from retinal images. In the research, I developed the proposed system on numerous convolutional neural networks and different architectures to improve the performance of the trained models. The comprehensive experiments were conducted on a diverse and well-annotated dataset, consisting of retinal images from patients with different eye diseases and healthy individuals.

Related Work

Image Classification

In the field of image classification, models are designed to take images as input and then categorize them into predetermined categories. Commonly used techniques for image classification include neural networks and convolutional neural networks, which have proven to be particularly effective in handling image data due to their ability to capture spatial features through convolutional layers. Image classification finds its application in various domains. For example, COVID-19 detection and face expression detection both use image classification. To be more specific, COVID-19 detection is diagnosing COVID-19 based on the x-ray image of the patient.

In the scope of this research, the aim is to apply image classification techniques to the field of retinal imaging. By utilizing an image classification approach, I will develop a model capable of accurately categorizing retinal images into relevant classes, thereby aiding in the diagnosis of various retinal diseases and contributing to advancements in ophthalmology.

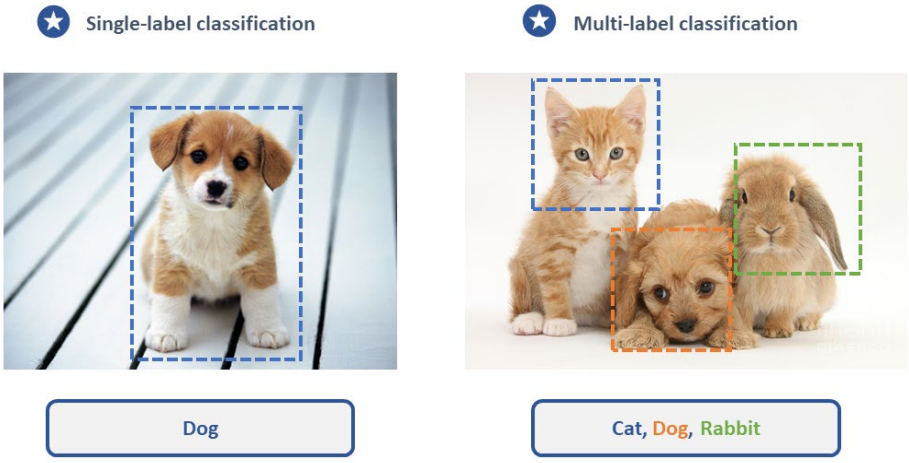

Figure 1. An example of image classification. (Javaid, 2023)

Retinal Image and Eye Disease

The retina, located in the inner layer of the eye, is a sensitive tissue that serves as the most advanced sensory organ of the human body and a part of the central nervous system. It converts incoming light signals into neural signals, altered by the brain through visual centers, and plays a crucial role in vision. Because the retina takes important roles in various fields and the fact that blood vessels are contained reflects the overall health, the retinal image is often exploited when detecting eye diseases. Among several methods used to capture the retinal image, fundus photography is the most commonly used method. Retinopathy, any damage or abnormal changes occurring in the retina of the eye, indicates symptoms of various eye diseases. For instance, retinal vessel caliber, vessel tortuosity, and microaneurysms are abnormal symptoms, which occur in certain conditions such as ocular melanoma and diabetes.

Eye diseases, including ocular melanoma, are often difficult to detect but can cause significant effects on one's health. Ocular melanoma, a form of primary cancer of the eye, creates melanin often on the back side of the eye, causing it to be difficult to detect. It appears as a pigmented mass on the retina, exhibiting irregular boundaries or shape. Diabetic retinopathy is a condition where blood vessels in the retina are damaged due to high blood pressure. Symptoms include blurred vision, floaters in the field of vision, and even vision loss.

Figure 2. An example of a retinal image and its acquisition process

Figure 2 demonstrates the process of taking a retinal image using a fundus/retinal camera. Doctors traditionally analyze retinal images of patients to detect abnormalities of the eye to diagnose eye diseases. However, this conventional diagnostic process is prone to errors, time-consuming, and subject to subjectivity. To address this problem, in this research, I develop a machine learning-based eye disease diagnosis system based on retinal images. Detailed information will be explained in Chapter 3.

Proposed Method

In this chapter, the proposed approach is explained in detail and serves as the roadmap for conducting the research. The system takes a retinal image as its input and produces target diseases as output. In this paper, I consider the proposed system as an image classification task since it classifies the retinal images into disease categories. In general, multi-class classification, resulting in one class, is the method commonly used. However, the proposed method is developed as a multi-label classification system, allowing the assignment of one or more labels, given that an eye disease is frequently followed by medical complications.

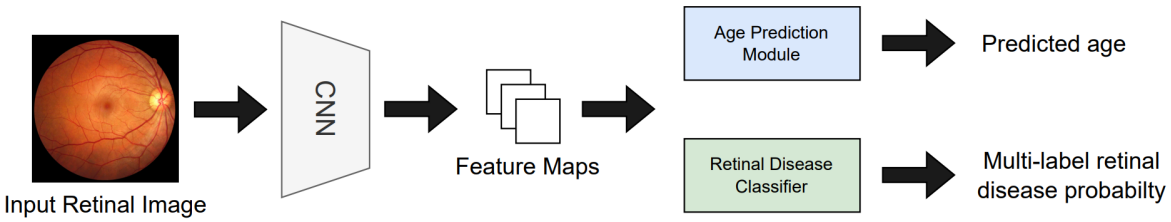

Figure 3. Overall architecture of the proposed method

Figure 3 demonstrates the overall architecture of the proposed method. The proposed model is composed of three modules: a feature extractor, *CNN*, age regression, *APM*, and disease classification, *RDC*. Firstly, the input retinal image, I, is fed to the *CNN*: $I \rightarrow map$ and output feature maps, *map*, which capture various visuals presented in the retinal image. The *map* is then passed through two separate modules, *APM* and *RDC*, resulting in *age* and P. Here, *age* and P denote predicted age and predicted retinal disease probability, respectively. Table 1 explains the notation used in this research. During the traditional diagnosis, the patient's age is an auxiliary information for ophthalmologists and has been proven to be related. The proposed method incorporates an age prediction module to enhance the performance.

Table 1. Notation used in this research

Original	Abbreviated
Retinal Image Input	I
Convolutional Neural Network	$CNN(.)$
Age Prediction Module	APM
Retinal Disease Classifier	RDC
Feature Map	map
Predicted Age	$\widehat{age}$
Target Age	$\widehat{age}_i$
Predicted Retinal Disease Probability	P
Loss of Age Prediction Module	L_{mse}
Loss of Retinal Disease Classifier	L_{ce}
Total Loss	L
True Positive	TP
False Positive	FP
False Negative	FN
True Negative	TN

In the proposed method, three functions are exploited to calculate the loss, a measurement of the difference between the predicted output and the ground truth, showing the performance of the module. *APM* utilizes Mean Square Error Function, while *RDC* employs Cross-Entropy Loss Function, tailored for the purpose of each module.

Equation 1: Mean Square Error Function

$$L_{mse} = 1/N \sum_{i=1}^{N} (age_i - \widehat{age_i})^2$$

Where, *N* represents the total number of the training, $\widehat{age_i}$, the ground truth in *i-th* term of the training sequence, and age_i , the predicted age during the *i-th* term, are subtracted. Every difference is squared and added, then the value is divided by *N*, resulting in the loss, *Lmse*.

Equation 2: Cross-Entropy Loss Function

$$L_{ce} = -log_e P$$

The Cross-Entropy Function measures the loss, *Lce*, by calculating the negative value of $log_e P$. In contrast to *RDC*, which leads to specific target diseases, *APM* results in a numerical value. This distinction endows *APM* with a regression task, while *RDC* gets a classification task. Consequently, the two modules employ different functions.

Equation 3: Total Loss

$$L = L_{ce} + \alpha \cdot L_{mse}$$

To compute the total loss, *Lce* and *Lmse* is added, where α is a decimal ranging between 0 and 1. Aligned with the objectives of our research, the performance of *RDC* assumes a nonessential part of the method. Thus, mitigate *Lmse* on *L*, thereby enhancing the accuracy of the proposed method. In this research paper, I set α to 0.8 as it yields the most accurate results.

Experimental Results

Dataset

To train and evaluate the proposed eye disease system, I use retinal disease dataset (Kaggle, 2019). The dataset contains 4876 samples in total, with 38 labels of disease and eye condition. For instance, it includes tessellated fundus, fundus neoplasm, and maculopathy for the label categories. Figure 4 shows the examples of the retinal disease images from the dataset, while Table 2 provides additional labels and explanations.

(a) (b) (c) (d) (e)

Figure 4. Examples of retinal disease image
(a): normal, (b): DR, (c): vessel tortuosity, (d): yellow-white spots, and (e): laser spots

Table 2. Disease label and explanation

Disease	Explanation

Normal	Labels a retinal image of a healthy patient.
Tessellated Fundus	Labels a retinal image with irregular depigmentation. Often associated with retinal disorders including myopia.
Large Optic Cup	The optic cup is a central area of the optic disc. Large optic cubes are caused due to the damage to optic nerve fiber, indicating the signs of glaucoma.
DR1, 2, 3	Labels a retinal image of a patient who has diabetes. Have cotton wool spots and hemorrhages, also known as blood loss, due to the damaged blood vessels from diabetes.
Possible Glaucoma	Labels a retinal image of a patient who has glaucoma. The image shows symptoms indicating glaucoma, which includes a large optic cup.
Optic Atrophy	Damage or degeneration of the optic nerve.
Severe Hypertensive retinopathy	Labels a fundus image of a damaged retina from high blood pressure. Swelling of the optic nerve head, cotton wool spots, and hemorrhages are the main symptoms of hypertensive retinopathy.
Disc Swelling and elevation	Also known as papilledema. Labels a retinal image with a swollen optic nerve heath.
Dragged Disc	Labels a retinal image of abnormally tilted optic nerve head. It is a symptom of retinal detachment.
Congenital Disc Abnormality	Labels a retinal image of an abnormal structure or growth of the optic nerve head. It has various forms and is congenital.
Retinitis Pigmentosa	Labels a retinal image of several deteriorated light-sensing cells, shown as dark pigments. It occurs rarely and is an inherited eye disorder.
Bietti Crystalline Dystrophy	Labels a retinal image of small deposits, looking similar to crystals. Similar to retinitis pigmentosa, it is a rare and inherited eye disorder that does not have a cure.
Peripheral Retinal Degeneration and Break	Labels a retinal image of damage and abnormal change on the outer side of the retina.
Myelinated Nerve Fiber	Labels a retinal image of myelin, which is a fatty substance covering the nerve fiber. It is shown as white colored patches and lines, similar to the cotton wool spots.
Vitreous Particles	Labels a retinal image with particles floating in the vitreous humor, a gel-like substance filling between the lens and retina. The particles have various appearances, such as dots and lines.
Fundus Neoplasm	Labels a retinal image with a tumor and abnormal growth of the fundus.

BRVO	BRVO stands for branch retinal vein occlusion. It labels a retinal image of blocked branch vessels and is associated with hemorrhage. Unlike CRVO, the bleeding occurs in a smaller region of the retina.
CRVO	CRVO stands for Central Retinal Vein Occlusion. It labels a retinal image of blocked vein and is associated with hemorrhage. The blood is widely spreaded compared to BRVO.
Massive hard exudates	Labels a retinal image with hard exudates. These are retinal deposits that often occur in diabetic retinopathy.
Yello-white spots-flecks	Labels a retinal image with spots of various types.
Cotton-wool spots	Labels a retinal image with a white area due to the disturbance of blood flow. It indicates several eye disorders, including diabetic retinopathy.
Vessel Tortuosity	Labels a retinal image of abnormally twisted and curved blood vessels. It is a sign of poor health conditions.
Chorioretinal atrophy-coloboma	Labels a retinal image of damaged and degeneration choroid and hole in iris, retina, choroid, or optic nerve.
Preretinal hemorrhage	Labels a retinal image of bleeding between the retina and vitreous humor.
Fibrosis	Labels a retinal image with scar tissues. It has light-colored patches and often leads to vision loss.
Laser Spots	Labels a retinal image of a patient who had laser therapy. It appears as equal-sized light-colored spots.
Silicon Oil in Eye	Labels a retinal image with silicon oil in the vitreous cavity. It is a treatment for several retinal conditions, especially retinal detachment.
Blur Fundus without PDR	Labels a retinal image of blurred visual representation. However, it is not caused by proliferative diabetic retinopathy(PDR).
Blur Fundus with suspected PDR	Labels a retinal image of blurred visual representation that share similar symptoms as diabetic retinopathy.
RAO	Labels a retinal image of a patient with retinal artery occlusion(RAO). It happens when the arteries of the retina are blocked.
Rhegmatogenous RD	Labels a retinal image with rhegmatogenous that is a type of retinal detachment. Often appears as white-colored layer separated from the
CSCR	Labels a retinal image of central serous chorioretinopathy. The central macula is changed by CSCR.

VKH Disease	VKH disease stands for Vogt-Koyanagi-Harada disease. It causes inflammation in tissues.
Maculopathy	Labels a retinal image with abnormal conditions affecting the macula.
ERM	ERM stands for Epiretinal Membrane, which is a thin layer of fibrous tissue that forms on the surface of the retina.
MH	Labels a retinal image with macular hole(MH). It may lead to central vision problems and distortion.
Pathological Myopia	Labels a retinal image of large white patches. It leads to inaccurate vision on distant objects.

Evaluation Protocol

For the evaluation protocol, I utilize k-fold cross-validation which is often conducted in many machine learning-based experiments. To effectively capture the performance and generalization ability of the proposed method, I segment the dataset into 5 folds. After conducting 5 different evaluation processes, the average accuracy and its corresponding standard deviation are calculated, each representing the overall performance and stability of the module.

Equation 4: Accuracy

$$Accuracy = \frac{True\ Positive + True\ Negative}{True\ Positive + False\ Negative + False\ Positive + True\ Negative}$$

Where true positive (TP) and true negative (TN) denote correct prediction of the model, and false negative (FN) and false positive (FP) indicate the incorrect prediction of the model, Equation 4 calculates the ratio of accurate prediction.

Equation 5: Precision

$$Precision = \frac{True\ Positive}{True\ Positive + False\ Positive}$$

In Equation 5, TP is divided by the sum of TP and FP, resulting in the ratio of the model's performance in the positive prediction it made.

Equation 6: Recall

$$Recall = \frac{True\ Positive}{True\ Positive + False\ Positive}$$

Recall equation calculates the model's performance in classifying the positive ground truth.

Equation 7: F1-score

$$F1\ Score = \frac{2 \cdot Precision \cdot Recall}{Precision + Recall}$$

In Equation 7, the overall accuracy is computed through dividing the product of 2, precision, and recall by the sum of precision and recall.

Performance Comparison

The experimental result, as illustrated in Table 3, demonstrates the exceptional performance of the proposed method.

Table 3. Performance of proposed method and state-of-the-art methods

	Accuracy	Recall	Precision	F1-score
AlexNet (Krizhevsky et al. 2012)	0.8081 (±0.0010)	0.8084 (±0.0010)	0.8081 (±0.0014)	0.8063 (±0.0011)
VGG19 (Simonyan et al. 2014)	0.8165 (±0.0011)	0.8177 (±0.0006)	0.8152 (±0.0008)	0.8142 (±0.0006)
MobileNetV2 (Sandler et al. 2018)	0.8174 (±0.0016)	0.8178 (±0.0011)	0.8167 (±0.0013)	0.8147 (±0.0010)
EfficientNet-B7 (Tan et al. 2019)	0.8227 (±0.0005)	0.8228 (±0.0012)	0.8207 (±0.0006)	0.8193 (±0.0007)
HRNet-40 (Wang et al. 2020)	0.8271 (±0.0011)	0.8279 (±0.0013)	0.8263 (±0.0005)	0.8246 (±0.0012)
Resnet-34 (He et al. 2016)	0.8301 (±0.0006)	0.8307 (±0.0011)	0.8292 (±0.0006)	0.8279 (±0.0016)
Proposed Method (Resnet-34 based)	**0.8427 (±0.0013)**	**0.8434 (±0.0012)**	**0.8417 (±0.0008)**	**0.8403 (±0.0010)**

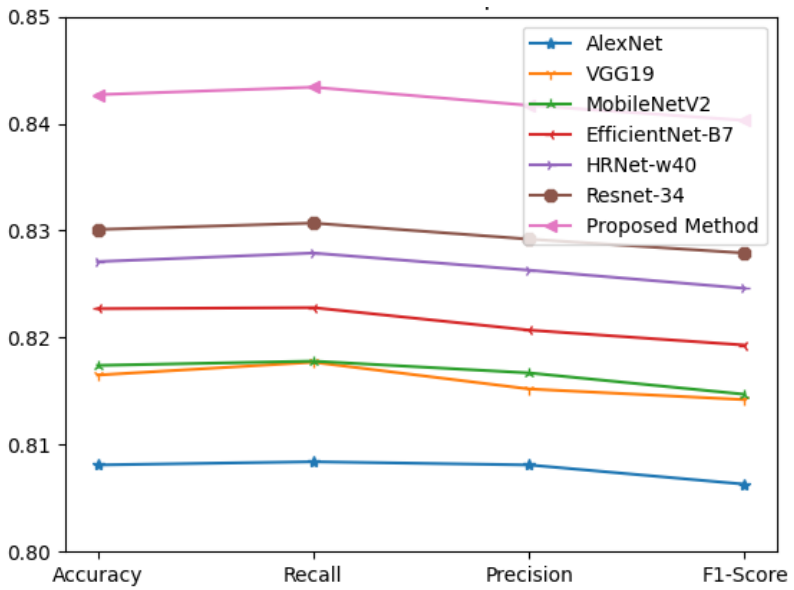

Figure 5. Performance comparison

The table 3 and figure 5 shows the performance, particularly accuracy, recall, precision, and F1-score, of six state-of-the-art methods and the proposed method. The overall performance of the state-of-the-art methods is evenly distributed within the range of 0.80 and 0.83, while the proposed method has an outstanding performance of 0.84.

Given the distinguished performance, to prove the contribution of *APM* to the increase, *APM* was applied to the state-of-the-art methods as shown in Table 4. The objective of this experiment is to establish the impact of *APM* on the overall performance, which has been proven to consistently enhance the performance of networks with different architecture.

Table 4. Ablation Study Result

	Accuracy (Ablation model)	**Accuracy (Full model)**
AlexNet	0.8081 (±0.0010)	**0.8133 (±0.0009)**
VGG19	0.8165 (±0.0011)	**0.8243 (±0.0012)**
MobileNetV2	0.8174 (±0.0016)	**0.8263 (±0.0011)**
EfficientNet-B7	0.8227 (±0.0005)	**0.8335 (±0.0009)**
HRNet-40	0.8271 (±0.0011)	**0.8386 (±0.0015)**
Resnet-34	0.8301 (±0.0006)	**0.8427 (±0.0013)**

Conclusion

In this paper, I proposed the accurate eye disease diagnosis system using convolutional neural networks. In order to enhance the performance, I introduced an age-guided approach. The experimental results demonstrate the outperformance of the proposed model, achieving state-of-the-art performance with an accuracy of 84%. To ascertain the efficacy of the age-guided approach, I also conducted an ablation study. The accuracy of several models has consistently increased, proving the contribution of the age-guided approach. In the future, I intend to implement the proposed model on the retinal camera's server and create an automatic eye disease diagnosis system.

Acknowledgments

I would like to thank my advisor for the valuable insight provided to me on this topic.

References

He, K., Zhang, X., Ren, S., & Sun, J. (2016). Deep residual learning for image recognition. In Proceedings of the IEEE conference on computer vision and pattern recognition (pp. 770-778). https://doi.org/10.48550/arXiv.1512.03385

Kaggle. (2019, Jun 18). "1000 Fundus images with 39 categories": Kaggle. https://www.kaggle.com/datasets/linchundan/fundusimage1000

Sandler, M., Howard, A., Zhu, M., Zhmoginov, A., & Chen, L. C. (2018). Mobilenetv2: Inverted residuals and linear bottlenecks. In Proceedings of the IEEE conference on computer vision and pattern recognition (pp. 4510-4520). https://doi.org/10.48550/arXiv.1801.04381

Shehmir Javaid. (2023, July 10). “Image Classification: 6 Applications & 4 Best Practices in 2023”: AI Multiple.
https://research.aimultiple.com/image-classification/

Simonyan, K., & Zisserman, A. (2014). Very deep convolutional networks for large-scale image recognition. arXiv preprint arXiv:1409.1556. https://doi.org/10.48550/arXiv.1409.1556

Tan, M., & Le, Q. (2019, May). Efficientnet: Rethinking model scaling for convolutional neural networks. In International conference on machine learning (pp. 6105-6114). PMLR.
https://doi.org/10.48550/arXiv.1905.11946

Krizhevsky, A., Sutskever, I., & Hinton, G. E. (2012). Imagenet classification with deep convolutional neural networks. Advances in neural information processing systems, 25.

Wang, J., Sun, K., Cheng, T., Jiang, B., Deng, C., Zhao, Y., ... & Xiao, B. (2020). Deep high-resolution representation learning for visual recognition. IEEE transactions on pattern analysis and machine intelligence, 43(10), 3349-3364. https://doi.org/10.48550/arXiv.1908.07919